Heliyon 10 (2024) e24021

Contents lists available at ScienceDirect

Heliyon

journal homepage: www.cell.com/heliyon

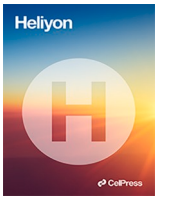

Research article

Modifying performance of solar still, by using slices absorber plate and new design of glass cover, experimental and numerical study

Abbas S. Shareef [a], Hayder J. Kurji [b], Ahmed H. Hamzah [c,*]

[a] Mechanical Department, Engineering College, Kerbala University, Kerbala, Iraq
[b] Mechanical of e Engineering, College of Engineering, Kerbala University, Kerbala, Iraq
[c] Mechanical of Engineering, College of Engineering, Kerbala University, Babylon, Iraq

ARTICLE INFO

Keywords:
W-shape of glass cover. slices absorbing plate.
productivity of solar still. six face cover.
Paraffin wax
Phase change material

ABSTRACT

By utilizing novel techniques on the absorber plates as well as the glass cover, this effort attempts to increase the distilled water productivity of a modified pyramid solar still. Under the climatic conditions of Iraq, the use of basin absorber plates with slices along its length, and a W-shaped glass cover was investigated experimentally and numerically. In this work, two comparable solar stills with basin absorber plates of 1 m2 have been planned and built using regional resources. Two absorber plates made of stainless steel were produced, first one was solid and the second was sliced. Two covers made of glass were produced one has a pyramid-shaped glass cover and the other a W-shape. According to experimental and numerical findings, forming slices and changing the glass cover resulted in a 20 % increase in the amount of distilled water. when compared to a pyramid glass cover and a standard sort of absorber plate.

1. INTRODUCTION

Three significant issues confront humanity at the start of the third millennium: food, energy, and water. Potable water is essential for human everyday living, yet there is currently evidence of a serious lack of this resource in some parts of the world. According to official statistics, it may also occasionally be of poor quality since a significant amount may be degrading as a result of inappropriate waste disposal and environmental circumstances. Since many people perish each year from water-related illnesses, access to clean water is essential for both national socioeconomic development and good health. Many diverse technologies, including reverse osmosis, have been implemented globally in response to the rising need for fresh water. But this sophisticated water treatment uses excessive amounts of traditional fuels and has detrimental effects on the environment. Solar desalination is the primary alternative to meet the population's needs for high-quality water with minimal input. This environmentally friendly method (solar process) can be thought of as a decentralized method of producing drinkable water, and it is a crucial job for rural communities. Solar distillation has the advantage of using sunlight energy as its source of power and having no fuel cost or carbon footprint. Its implication promises residents of remote areas a better quality of life and economic growth. As the energy from the sun's radiation grows with surface exposure, it demands more area as retaliation. Depending on the requirements, solar distillation systems can be multi-scale. Although a single family can produce a few liters of clean water per day, significantly larger amounts are being made accessible for agglomeration by using low-cost technology systems like glass in greenhouse-like structures atop brackish water basins. Consequently, it is crucial to

* Corresponding author.
E-mail addresses: abbas.al-rakabi@uokerbala.edu.iq (A.S. Shareef), hayder.j@uokerbala.edu.iq (H.J. Kurji), e.ahmed2131987@yahoo.com (A.H. Hamzah).

https://doi.org/10.1016/j.heliyon.2024.e24021
Received 3 August 2023; Received in revised form 20 December 2023; Accepted 2 January 2024
Available online 7 January 2024

conduct several studies at both the academic and industrial levels in order to support the desalination process. Since the energy source is only dependent on the accessibility, effectiveness, and gratuity of solar energy, solar desalination is the ideal method for overcoming the scarcity of potable water in dry places, especially for impoverished towns. In remote locations, several developed solar desalination devices work effectively as solar stills. Numerous studies on this topic were initially conducted through experimental investigations to evaluate the usefulness of each recognized distillation solar system. The first step was the creation of straightforward traditional solar stills. The basic building block of a solar still is a clear plastic or glass container that is surrounded by a simple basin filled with salt water. Water is heated by the sun's energy to the point of evaporation. Purified water is collected in troughs after distillation on the cool cover's inside surface.

In the context that follows, numerous studies have been strongly encouraged to use solar distillation stills to demonstrate their exceptional impact in the field of producing drinkable water. These pieces also provide excellent case studies for understanding the transition from traditional stills to modifying stills.

one of the crucial elements in boosting the solar distiller, if not the most important, is the water basin, as the increase in the area of this part leads greatly to enhance the heat absorbed, and as a result, this heat is transferring to the water, increasing the rate of evaporation. Improvements in evaporating surface area boost a solar still's production [1]. studied expanded surfaces by combining fins into a solar still and used jute cloth to speed up evaporation. It is necessary for the basin to absorb the majority of the energy reached to the still, convert it to heat, then disperse it into the salty water. Give the greatest area of surface for evaporation. Additionally, it must to keep any surplus heat and employ it when the intensity of radiation reduces [2]. conducted theoretical and experimental research on fin material's impact on finned basin stills' production. Findings revealed that gender metal fins have little effect on still productivity.

The still's cover is a critical component in the effective construction of the solar still unit. Sunrays strike the glass first, then travel to the solar still, where they evaporate salty water to produce consuming water. Right design of the cover is a critical aspect for increasing solar still productivity. As a result, modifying the cover conditions improve the performance of this type of still. Several factors affect the efficiency and productivity in terms of shape and materials, including the outer cover of the solar distiller. The top cover is made to let in and transfer as much radiation into the still as it can. The cover should also be able to condense the most water vapor while releasing the least amount of heat into the atmosphere. Radiation is sent and received by the still through the transparent cover. At its bottom surface, condensation also takes place. Additionally, it should lessen heat radiation entering the atmosphere, Glass is the best choice for this mission [3]. Also investigate how cover materials affect the heat and mass transfer coefficient and, consequently, the still's productivity. One still's condensing surface was a glass surface, whereas the second still's had an plastic cover that was 3 mm thick. The plastic solar still with the glass cover produced 30–35 % more output than the plastic sun still with the Plexiglas cover for water depths of 10 cm [4]. conducted an experiment on pyramid still productivity, they discovered that as compared to traditional still, the output of pyramid still rose by 25 % [5]. explored a pyramid type still's behavior experimentally. According to the findings, the pyramid still uses less energy than the regular still.

Consequently, glass was chosen as the material for this project. The tilt of the cover is altered to direct gathered condensate down the drain and into the basin. Sun energy and condensation rate have an impact on how much condensate mass accumulates [6]. conducted an indoor modeling experiment and found that a covering with an inclination of thirty degrees' increases production rate. In this article, the inclination of the walls of the upper cover was chosen to be identical to the latitudes of the city of Hila, which are 32.2°. The glass must endure its own weight as well as temperature stresses. need more thickness glass wall will be used for greater surface area. Yet, as glass gets thicker, less heat and radiation can pass through it. A result of condensation on a layer at the bottom surface, the transmittance loss at the cover is smaller. Wind's speed has an impact on outside glass temperature as well. Because of increased transfer of heat by convective through the glass to the atmosphere, the still's productivity rises with higher wind speeds [7]. In order to evaluate and verify the numerical and experimental findings of different glass cover designs, energy balance equations were used. Finally, two months of results from two different glass covers on two identical area solar stills were compared to determine the increase in efficiency. as a result, new design glass cover chosen in this article. Efficiency is greatly influenced by the gap between glass and the water, as increasing distance reduces productivity and vice versa. As a result, in this study, two different shapes of glass covers were found by correlation.

The goal of the current study is to increase the productivity of the solar still by adding two technologies. The first is related to changing the design of the upper cover, whereby the gap between the surface of the salt water and the inner cover of the glass was reduced from 1245 cubic meters to 1112 cubic meters.

The second technique is related to changing the shape of the absorber plate from solid to slit to increase its surface area by 20 %.

2. Experiments

Two rigs are designed and manufactured with typical dimensions and specifications of the materials, the salt water basin which it is manufactured from food grade stainless steel 304 with a thickness 2 mm as in figure (1A). To increase the surface area of the absorber plate, we made Slices along its with a depth 1 mm and a width 2 mm, and distance between one slice and another was 1 cm, so that the total number of these slices was 90, and The percentage increase in the area of the absorber pale is 20 %. as in figure (1E). The height of the walls of the salt water basin is 5 cm. Output of the still is gathered using a U channel that is positioned at the base of the still's slanted glass side. To prevent energy loss from the water basin, there is 5 cm glass wool insulation. Raw water is delivered to the solar still using a 500 kg size brackish water storage tank. Each solar still has a valve for control attached to keep the water flow inside the still constant at 3 cm. 5 cm insulation are used around basin to decrease heat loss from the bottom and sidewalls of basin as in figure (1B).

2.1. Glassing

The glassing cover Consists of six pieces of glass, 4 mm thick. The front and rear piece measures (100 × 51 × 51 × 34) cm, while the two sides piece (W- shape) measures (100 × 51 × 26 × 26 × 51) cm. The two upper pieces are as an irregular rectangle (34 × 26 × 26 × 68) cm, all cover pieces are oblique at an angle of 32° with the horizon, to form a cover as an incomplete pyramid inclined to face the sunlight at all times figure (4.1C, D) shows the shape of new design and traditional glass covers. The goal of choosing this shape is to reduce the gap between the surface of the salt water and the inner surface of the glass while maintaining the same condensed surface.

3. Experimental setup

To study effects of change design of glass cover, and increase absorber plate, an experimental facility has been created and built in Babylon City, Iraq (Latitude 44.4 and Longitude 32.2) (see Fig1a). For both the standard pyramid and the modified pyramid, Throughout the working days, the elevation Figb of water remains constant at water basin at 3 cm. During the months of March and April 2023, work begin at 7:00 a.m. and end at 6:00 p.m. During the experiment, the following variables were measured hourly: solar radiation, wind speed, ambient air, inner and outer glass temperature, basin water temperature, absorber temperature, and hourly distillate yield. Fig. 4 shows the photo of both the experimental devices.

4. Heat-flow analysis

This section presents the thermodynamic analysis's equations.

4.1. Energy assessment

According to the first law of thermodynamics, the energy balancing equation is given by:

$$\mathrm{Ein} + \mathrm{Ege} = \mathrm{Eout} + \mathrm{Est}$$

For energy analysis, the following presumptions are taken into account (El-Sebaii and Khallaf 2020).

- The salinity of the water is kept consistent at 3 cm.
- No water vapor leakages occur in solar stills.
- A quasi-static model of the whole thing is taken into account.
- A solar still's basin is insulated to lessen conductive heat loss.
- The overall coefficients of heat transfer are linear functions of temperature.
- Glass and salt water's thermo-physical characteristics are taken to be constant.
- The basin of the solar still is being directly hit by solar radiation.
- Saline water has a higher transmission and a low absorptive.

According to **Elango et al. (2015),** the following equations provide the energy balances for different solar still components:
Basin:

$$h_3\,(T_b - T_w) = M_w\,C_w\,\frac{dT_w}{dt} + h_1\,(T_w - T_{gin}) \tag{1}$$

Graphite plate fins:

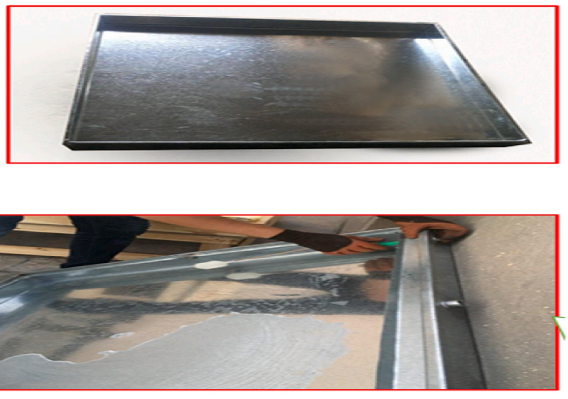

Figure 1a. Water basin.

Figure 1b. glass wool insulator and wooden frame.

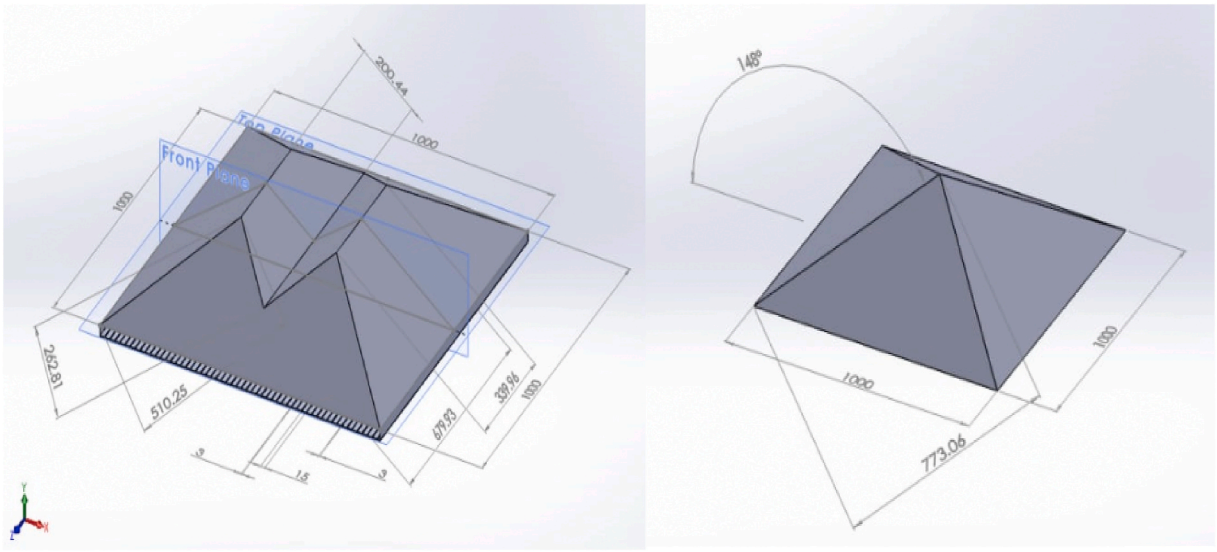

Figure (1C). Glass covers for W-shape and pyramid covers in sold work

Figure (1D). Glass covers for W-shape and pyramid covers, experimental photo

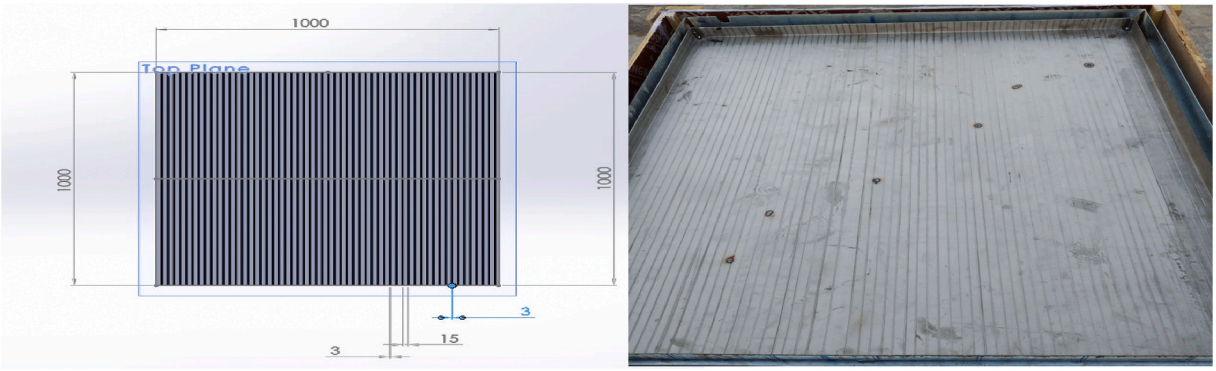

Figure (1E). slices absorber plate sold work experimental, photo

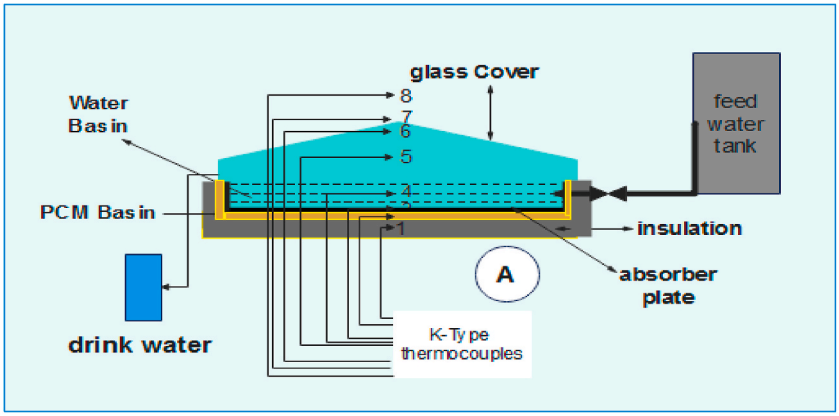

Figure (2). schematic diagram of traditional solar still with thermocouples.

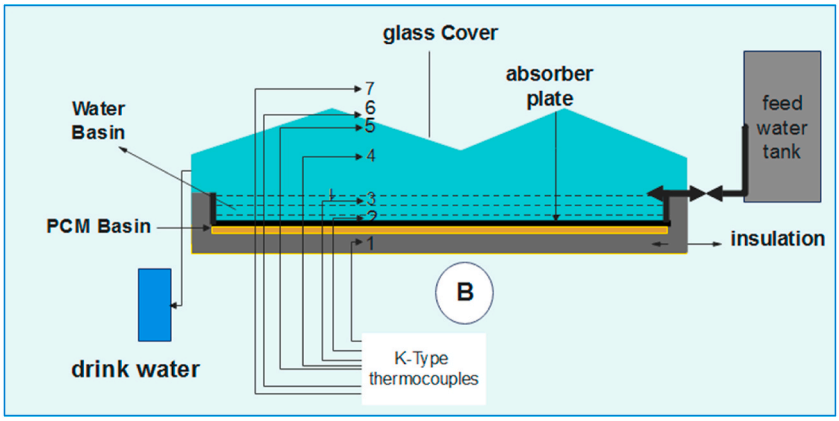

Figure (3). schematic diagram of modified solar still with thermocouples.

$$\frac{Kgp}{Xgp}\left(T_b - T_{gp}\right) = \frac{Kin}{Xins}\left(Tgp - Ta\right) + MgpCp,gp\ \frac{dTgp}{dt} \tag{2}$$

The balance of the energy of the liner (nanoparticles) of the basin is:

$$\alpha_b I(t) = h_3(T_b - T_w) + h_{bc}\left(T_b - T_{pcm}\right) \tag{3}$$

Basin with graphite panel:

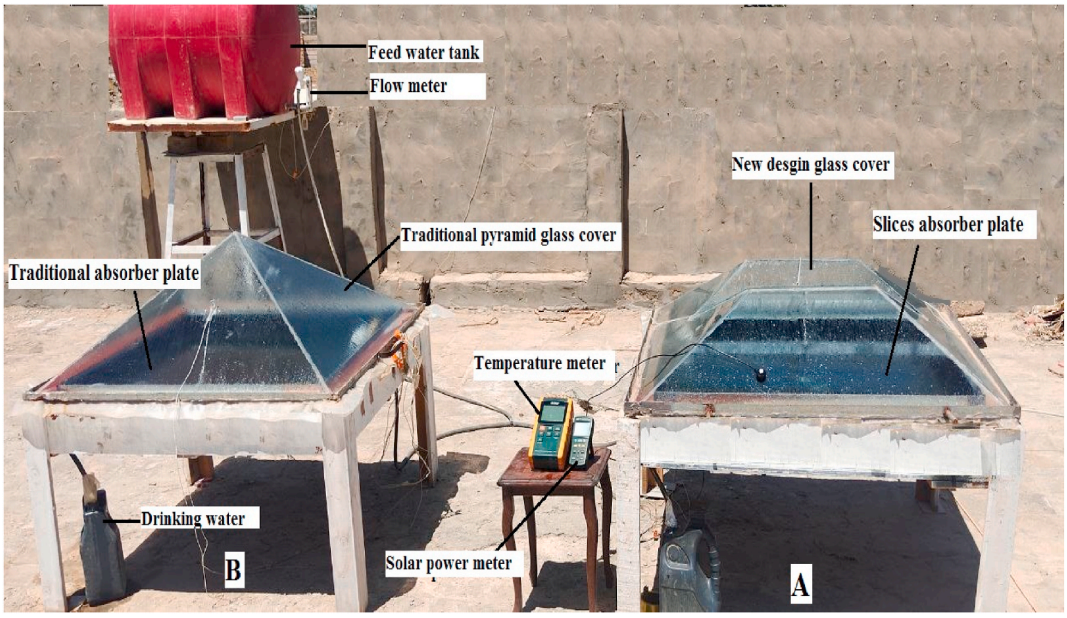

Figure (4). photo of a new design, Conventional solar still.

$$\alpha_b \tau g \tau w \, I(t) Ab = \frac{Kin}{Xins} \, (Tgp - Ta) + MgpCp, gp \, \frac{dTgp}{dt} \tag{4}$$

The balance of the energy of the PCM is:

$$h_{bc}\left(T_b - T_{pcm}\right) = M_{b\ cpb} \, \frac{dTgp}{dt} \left(\frac{dT_b}{dt}\right) + h_{c\ b-w}\left(T_{pcm} - T_a\right) \tag{5}$$

The hourly and daily solar still productivity is:

$$m_{ew_h = h_{ew}} \left(T_w - T_{gin}\right)/\gamma \tag{6}$$

$$m_{ew_d = \sum_{24\ hr}} m_{ew_h} \tag{7}$$

Solar still efficiency is:

$$\eta_i = \frac{h_{ew}\left(T_w - T_{gin}\right)}{I(t)} \times 100\% \tag{8}$$

The details of parameters in equations are described:

$$h_1 = h_{cw} + h_{ew} + h_{rw} \tag{9}$$

$$h_{cw} = C \, \frac{K_f}{d} \, Ra_f{}^n \tag{10}$$

$$Ra_f = Gr_f \, Pr_f, Gr_f = \frac{d^3 \, \rho_{fg}^2 \, \beta \Delta T'}{\mu_f^2}, \; Pr_f = \frac{\mu_f C_f}{K_f} \tag{11}$$

$$\Delta T' = \left[\left(T_w - T_{gin}\right) + \frac{\left(P_w - P_g\right)\left(T_w + 237.15\right)}{26800 - P_w}\right] \tag{12}$$

$$P_w = e^{\left(25.317 - \frac{5144}{T_w + 237.15}\right)}, P_{gin} = e^{\left(25.317 - \frac{5144}{T_{gin} + 237.15}\right)} \tag{13}$$

$$h_{ew} = 16.273 * 10^{\cdot 3}\left[h_{cw}\left(P_w - P_g\right) / \left(T_w - T_{gin}\right)\right] \tag{14}$$

$$h_2 = h_{ca} + h_{ra} = 5.7 + 3.8V \tag{15}$$

5. Numerical solutions

This section explains the software that simulates heat flow into and built, including its components. Fluent, a division of Ansys, is the program utilized in the current project (version 2016 R1 of Workbench). It was utilized to determine the daily efficiency of water distillation as well as the numerical solutions for water temperatures within the solar system. Because it delivers more precise results and is more in line with experimental findings, this software was chosen for the current task. It can also resolve the mass, momentum, and energy conservation equations. This applies to a variety of situations, including fluid flow in two or three dimensions, constant or erratic state (transient), compressible or incompressible fluid, and others. Additionally, it has been used to other study areas, including the subject of heat transfer (the area of the present work).

5.1. Geometry of test section

SOLIDWORKS 2016 is utilized to develop all complex and simple engineering forms for the solar distillation system's three-dimensional testing model (see Table 1). Two testing models were created; the X–Y plane was first chosen to sketch the fundamentals of the initial test model. The extrude order was supplied for geometry to get the 3D structure as a full pyramid; the first model was completed at this stage. To create the second prototype, the same steps were repeated in the first model, and then the upper peak was extruded and cut on the front side. The walls on all sides of the structure were designed to be adiabatic, and it is tilted at an angle of 32^{o}. The bottom surface of the testing prototype represented the vapor entry points into the test area, while the top surface simulated the glass cover. The geometric dimensions are the same as in the experimental design. Figure (5) represents the first model, which is the complete pyramid shape. As for figure (6), it represents the new design of the upper cover of the solar distiller. Tables 2 and 3 represent the Specifications of the Geometry for two model.

5.2. Mesh Generation

The mesh or grid creation process is the second step in the building of the computer Fluent software. The test section's mesh (the test domain) is constructed following the construction of the test model's geometric design. In other words, the examination section is broken down into its most basic components. There are various grid types, and selecting the best one requires consideration of elements geometry or flow field, etc. Grid size and kind greatly affects the amount of CPU (central processing unit) time required, how quickly convergence occurs, and how accurately results are produced.

The present work's mesh type is quadrilateral, and the size of element is (1 mm^2). The tetrahedral of the computing grid. This result was reached following a number of tests using grids of various types and sizes under the identical boundary circumstances. In comparison to other mesh types and sizes, the (1 * 1 * 1) mm quadrilateral mesh yields the best results. Table (4) is a list of the mesh's features. The test section's grid of the two form flow is depicted in Figures (7) for two stills. It can be noted that the number of elements and nodes in the old or traditional design are more than the new design because the area is smaller in new one.

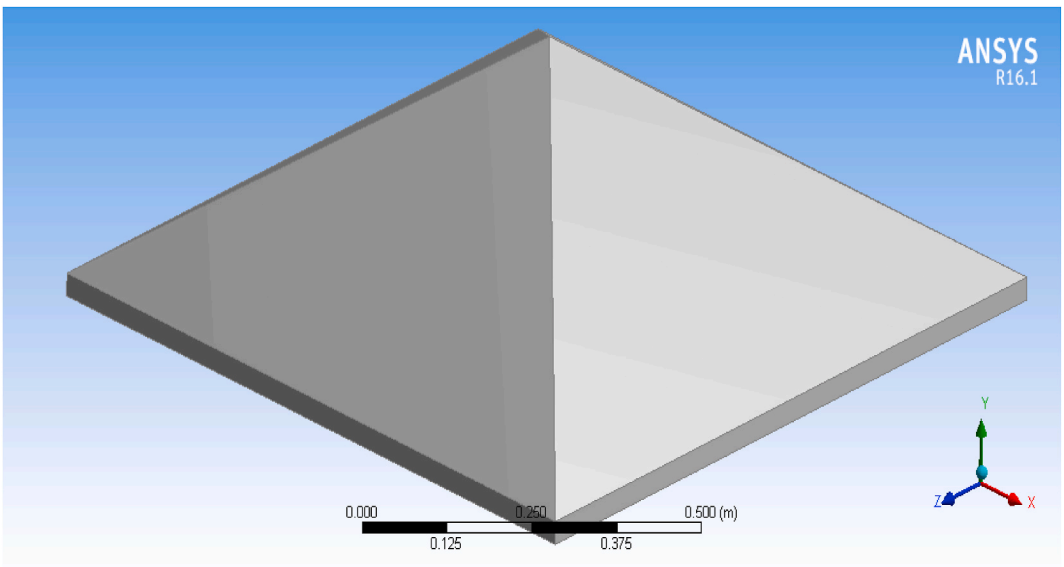

Figure (5). 3D Model of pyramid Solar Still.

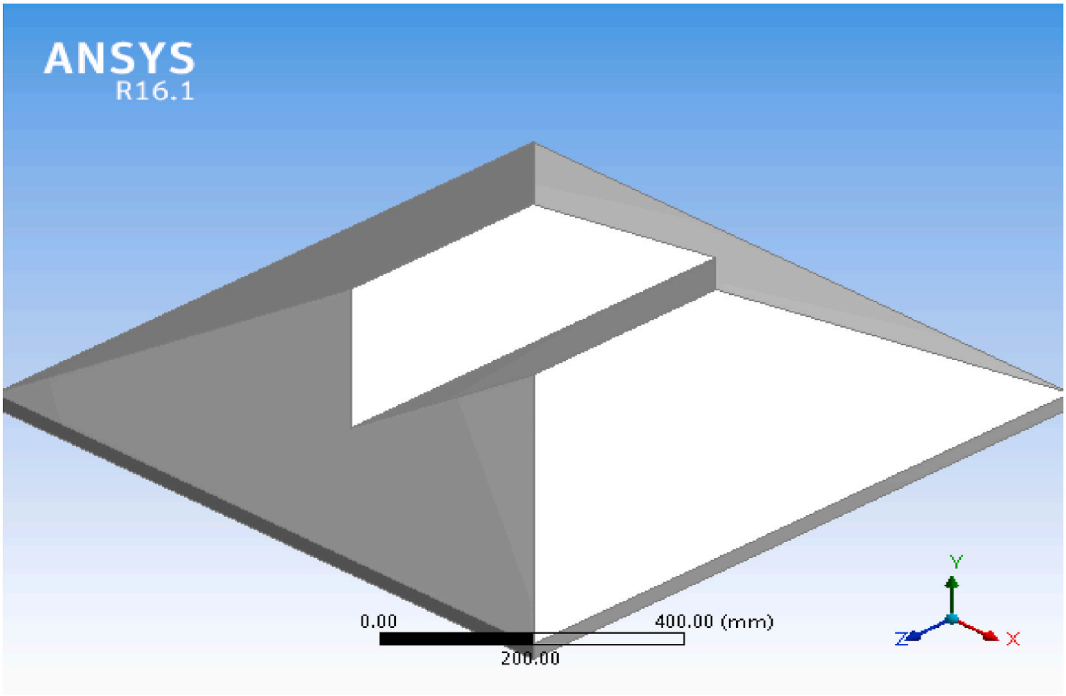

Figure (6). 3D Model of new design Solar Still.

Table 1
Comparison between traditional and modified distillates.

Parte	Traditional SS	Modified SS
brackish water basin	Solid absorber plate. Material: plate Stainless Still/304	Slices absorber plate. Material: plate Stainless Still/304
Surface area of absorber plate	1 m^2	1.2 m^2
glass cover	Pyramid shape with 4 pieces	W-shape with 6 pieces
Gap volume	1.245 m^3	1.112 m^3
Wooden box, Insulation, and Stand	The same	The same
schematic diagram	Fig. 2	Fig. 3

Table 2
shows the Thermophysical and radioactive characteristics of solar still materials. (Dhivagar et, al.)

NO	Property	Magnitude
1	Absorptivity of the Glass cover (α_g)	0.05
2	Saline water absorptivity (α_w)	0.05
3	Basin absorptivity (α_b)	0.9
4	Quantity of saline water (m_w)α_b)	20.5 kg/m^2
5	Quantity of glass cover (m_g)α_b)	10.1 kg/m^2
6	Quantity of basin (m_b)α_b)	15.6 kg/m^2
7	Saline water transmissivity (τ_w)	0.95
8	Glass cover transmissivity (τ_g)	0.9
9	Saline water–specific heat (C_{pw})	4.178 kJ/kg.K
10	Glass cover–specific heat (C_{pg})	0.8 kJ/kg.K
11	Basin-specific heat (C_{pb})	0.48 kJ/kg.K
12	Effective emissivity (ε_{eff})	1
13	Thermal conductivity of basin (k_b)	16.3 W/m^2.K
14	Thickness of basin (x_b)	0.002 m
15	Thermal conductivity of water (k_w)	0.57 W/m^2.K
16	Thickness of water (x_w)	0.03 m
17	Thermal conductivity of Insulating material (ki_{ns})	.039 W/m^2. K
18	Thickness of insulation (x_{ins})	0.05 M
19	Salinity-to-basin heat transfer coefficient ($h_{c\ b-\ w}$)	135 W/m^2.K
20	total heat transfer coefficient between a basin and the surrounding air	14 W/m^2.K

Table 3
The Specifications of the Geometry for two model.

Properties		Pyramid design	New design
Program Generation		SOLIDWORKS 2016	SOLIDWORKS 2016
Volume		1.245 m^3	0.112 m^3
Fluid/Solid		Solid	Solid
Analysis Type		3-D	3-D
Bounding Box	Length X	1000. mm	1000. mm
	Length Y	342.43 mm	236.22 mm
	Length Z	1000. mm	1000. mm
Dimensions	Centroid X	1.2393e-017 m	2.3724e-018 m
	Centroid Y	5.7286e-002 m	4.4067e-002 m
	Centroid Z	1.6165e-018 m	−2.9655e-018 m

Table 4
Characteristics of the mesh for tow solar still.

Object Name	Mesh	Pyramid design	New design
Physics Preference		CFD	CFD
Solver Preference		Fluent	Fluent
Relevance		100	100
Sizing	Use Advanced Size Function	Curvature	Curvature
	Relevance Center	Fine	Fine
	Smoothing	High	High
	Transition	Slow	Slow
	Span Angle Center	Fine	Fine
	Curvature Normal Angle	Default	Default
	Min Size	1.6706e-004 m	1.6706e-004 m
	Max Face Size	4.0 mm	4.0 mm
	Max Size	4.e−002 m	4.e−002 m
	Growth Rate	Default(1.1) mm	Default(1.1) mm
	Minimum Edge Length	30.0 mm	30.0 mm
Nodes		318935	210150
Elements		1446419	1108350
Mesh Controls	Scoping Method	Geometry Selection	Geometry Selection
	Method	MultiZone	MultiZone
	Mapped Mesh Type	quadrilateral	quadrilateral
	Scoping Method	Geometry Selection	Geometry Selection
	Free Face Mesh Type	Tetra/pyramid	Tetra/pyramid

5.3. Setup and solution

5.3.1. Boundary conditions

In this study, water is treated as the primary phase and water vapor as the secondary phase. The boundary conditions for the mathematical model utilized in the current study were split into three categories: inside and outside of the solar distiller, as well as at the walls of the distiller.

The inside boundary conditions are shown (Solution Initiation) in Table (5) (see Table 6).

The boundary conditions were established at the outside temperature and pressure parameters for the solar distiller.

5.4. CFD POST

5.4.1. The temperature contour

Figures (8,9) depict the temperature variation contours for two-phase flow using solar still test at 12:00 p.m. The distributions of temperatures of the distiller with traditional pyramid cover, and distiller with W-shape cover and slices absorber plate. It can be observed that the temperature of the advanced distiller is higher than that of the traditional one. The reason for this increase is the increase in the surface area of the absorbent plate and the smaller size of the gap. The Ansys program shows the superiority of the advanced still over the traditional one, as the temperature of the glass for the first ranges between 53 and 54CO. In contrast, the temperature for the traditional still is 44–45 C^O.

5.4.2. The velocity vector

Figures 10 and 11 present the velocity vector at the time 12:00 p.m. for pyramid, W-shape glass cover, which indicate the direction of velocity. It can be noted from these figures that the velocity vector is formed as vortices. The upper layer evaporation of the water basin generated vapor and moved in vortices in a vacuum. The buoyancy force's impact causes the warm vapor to rise to the top. Water droplets will condense at the top of the vapor and fall down with the incline of the glass cover. The Ansys program showed an increase

Table 5
Steps of computational fluid Dynamic by using Ansys-Fluent software.

Start CFD Fluent			
Geometry	Table 3		
Mesh	Table 4		
Setup	Model	Multiphase	Volume of fluid: 3
		Energy	On
		Viscose	K-epsilon
		Radiation	DTRM
	Material	Fluid	Air
			Water- liquid
			Water- vapor
		Solid	Glass
			Wood
			Steel
	B.C	Glass	Thermal: convection
			Radiation: semi- transfer
		Walls	Thermal: convection
			Radiation: adiabatic
		Absorber plate	Thermal: heat flux
			Radiation: adiabatic
	Solution method	SIMPLE	
	Solution Initiation	Volume fraction of water& vapor: 0.001,0999	
		Inlet Water temperature: 45.8 C^o	
		Reference pressure: 1 atm	
		Reference density: 1.225 kg/m^3	
	Run calculation	8000 iterations: fig. 3.5	
Solution	Calculation complete: solution is converged: fig. 3.6		
Results	Temperature contour	Chapter five	
	Velocity stream		
	Vapor fraction		
End			

All of the sides were set as thermal conductor walls for the boundary conditions at the solar distiller walls.

Table 6
Comparison of the efficiency of the current study with earlier works done in other places.

Ref.	Author	Country, year	Solar type	Emprovmant	Efficiency %
10	S.Rashidi et al.	Egypt, (2017)	single slope SS	reticular porous	17.35
11	H. Panchal et al.	India 2012	single slop SS	increase area of absorber plate by using fins	25
12	Velmurugan et al.	India 2021	single slop SS	using fins inside the SS basin	49.5
13	N. Abdelal et al.	Jordan (2017)	pyramid SS	carbon fiber/nanomaterial absorber plate	30
14	Alaian et al.	Egypt, (2016)	single slope SS	pin-finned absorber plate	55
Curent study	A.Hassan et al.	Iraq, (2023)	pyramid SS	New shape of glass cover, increase area of absorber plate	73
15	A.E. Kabeel et al.	Egypt (2017)	pyramid SS	v-corrugated absorber plate with PCM	87.4

in the velocity of water vapor in the solar still, thus increasing the amount of steam condensing on the surface of the inner glass.

5.4.3. The volume fraction

Figures 12 and 13 Show the condensation of water drops at 12:00 p.m. on the glass lid's interior surface of conventional, and new design still. It is suitable for water droplets condensed so by putting the contour between zeros and (1 × 10-3). The side view of the system and the outlines of the water fraction in volume that matches the bottom are shown, the phases of liquid and vapor are entirely separate, and the surface interface is distinctive. It can be seen a larger amount of liquid state on the inner surface of the cover of geometry for the developed distiller, As a result, its productivity is greater than that of traditional distillers.

6. Experimental results

Figure (14) displays ambient temperatures and sun radiation. This chart illustrates how the sun's rays and ambient temperature peak at noon and then begin to decline. Figure (15) shows the basin's water temperature. The modified pyramid still and the conventional pyramid still both have a maximum water temperature in the basin of 1:00 p.m. is $69.5C^0$, $60C^0$ respectively. This result shows that the modified still's basin temperature is greater than the standard pyramid still's because the gap between Fig 16 the water and upper cover is less, and the slices absorbing plate can absorb more energy because it works as fins. Figure (18) Show the inner glass temperatures for both stills. As could be seen, the modified pyramid still's maximum inner glass temperature at 1:00 p.m. was $54.8C^0$, while the regular pyramid still's was $47.2C^0$ (see Fig. 17) (see Fig. 19).

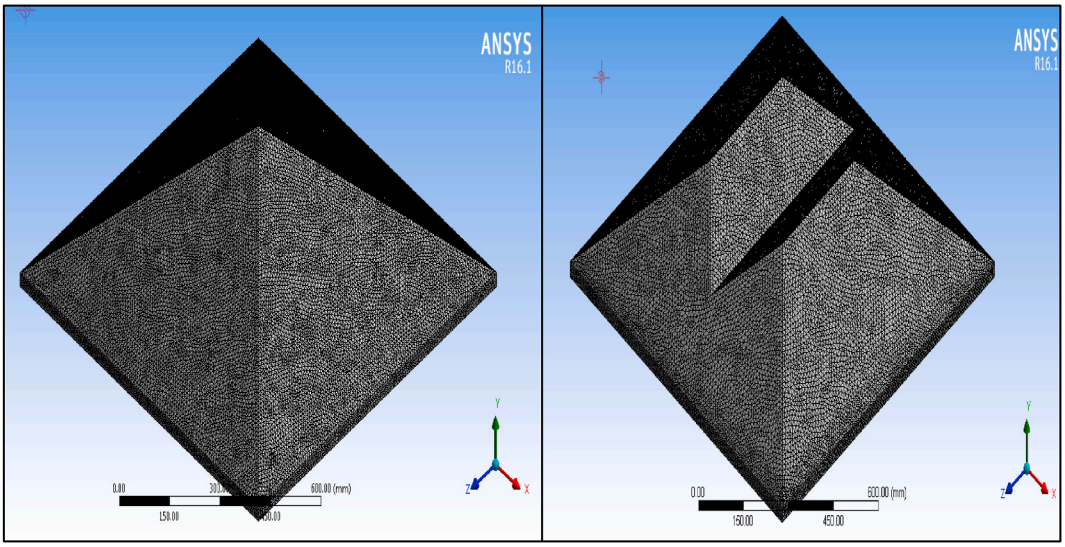

Figure (7). 3D mesh for traditional pyramid, new design still.

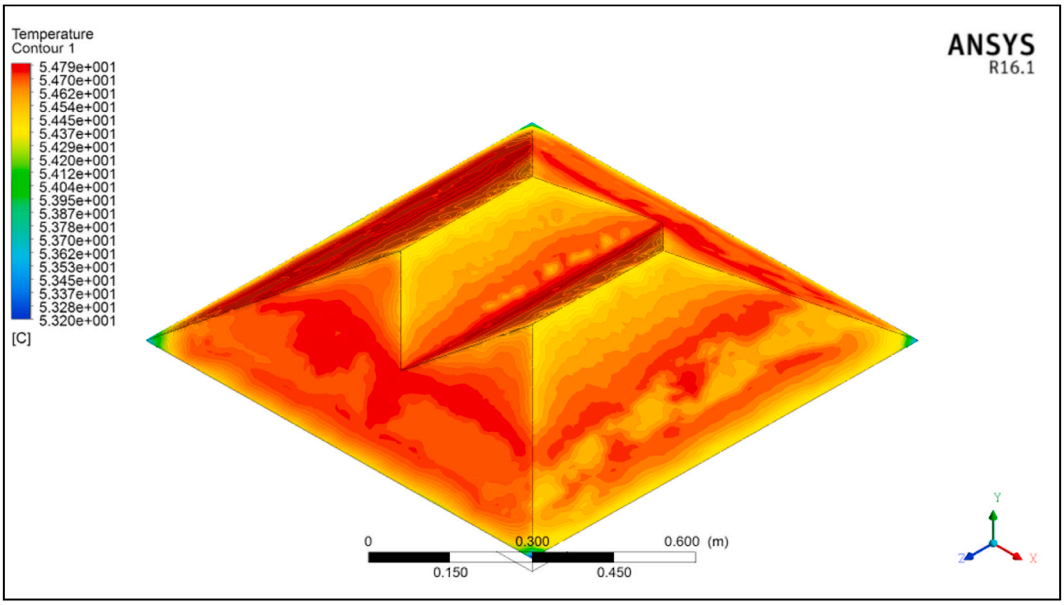

Figure (8). Temperature contour for modifying design still at 12:00 p.m.

Figure (20) demonstrates how the output of pure water rises progressively until it reaches a high at 1:00 p.m. The variation in temperatures between the aquarium's water and the outside of the glass enclosure, which is largest now, affects them (evaporation and condensation). Compared to the conventional one, the new design solar distiller is more productive, as the productivity of the developed solar distiller reached 4.4 l m^{-1} d^{-1}, in contrast, the productivity of the traditional distiller is 2.6 l $m^{-1}d^{-1}$.

Figure (21) show the hurly efficiency for both types of solar still, the maximum efficiency for traditional pyramid still is 54 %, while the efficiency for modified still is 73 %.

The results of the practical part of the experiment showed consistency with the theoretical aspect, as the developed distiller excelled in terms of temperature, productivity and efficiency.

7. Validation with previous work

To verify the experimental solution, the calculated value of efficiency. It is essential to calculate the efficiency, and weighed against the experimental findings of the prior study made by different researcher [10–15]. The research that was taken for the purpose of

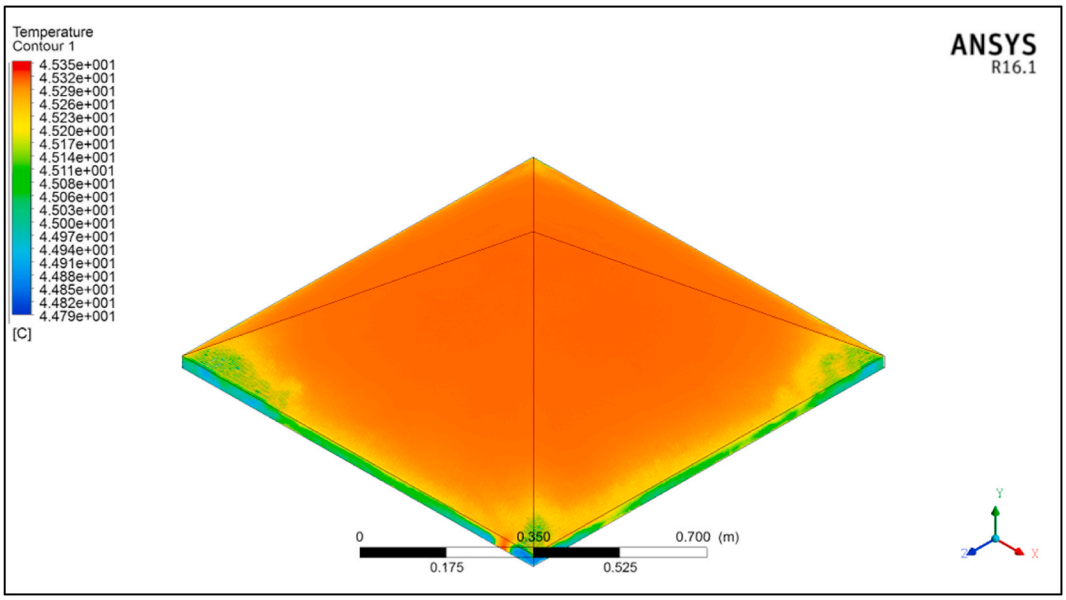

Figure (9). Temperature contour for Traditional design still at 12:00 p.m.

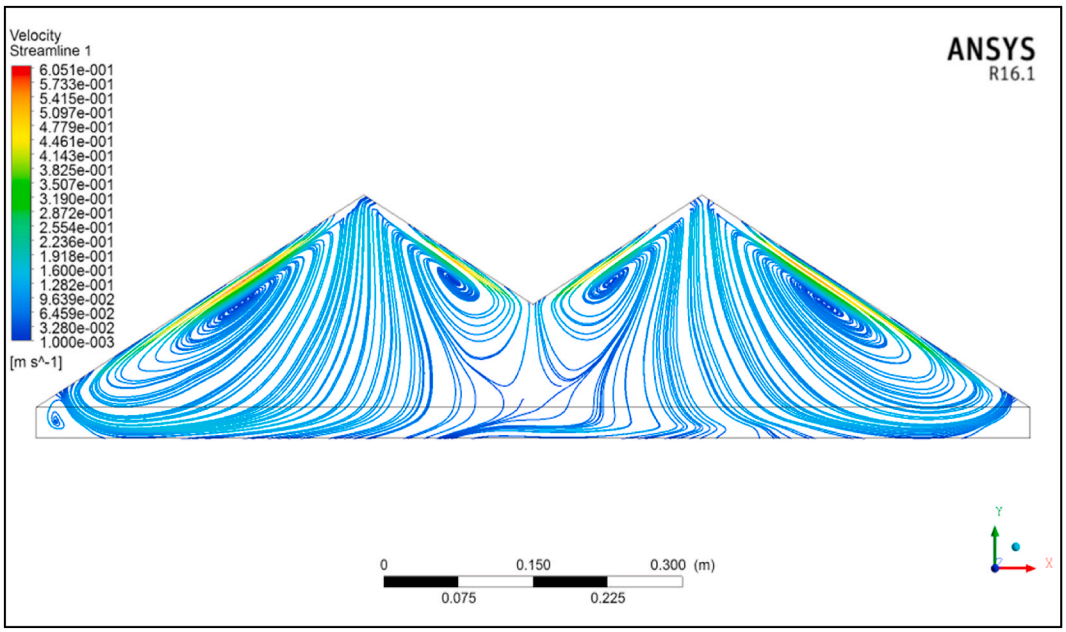

Figure (10). streamline contour for modifying design still at 12:00 p.m.

comparison studies the effect of fins, considering that they increase the surface area of the absorbent plate, and also models were taken related to studying the effect of the glass cover.

8. Conclusions

Solar stills are practical since they are easy to operate, can provide fresh water to isolated locations where there isn't any, and their environmental friendliness makes them an appealing technology in the future.

Following conclusions were drawn from the current work's experimental and numerical findings.

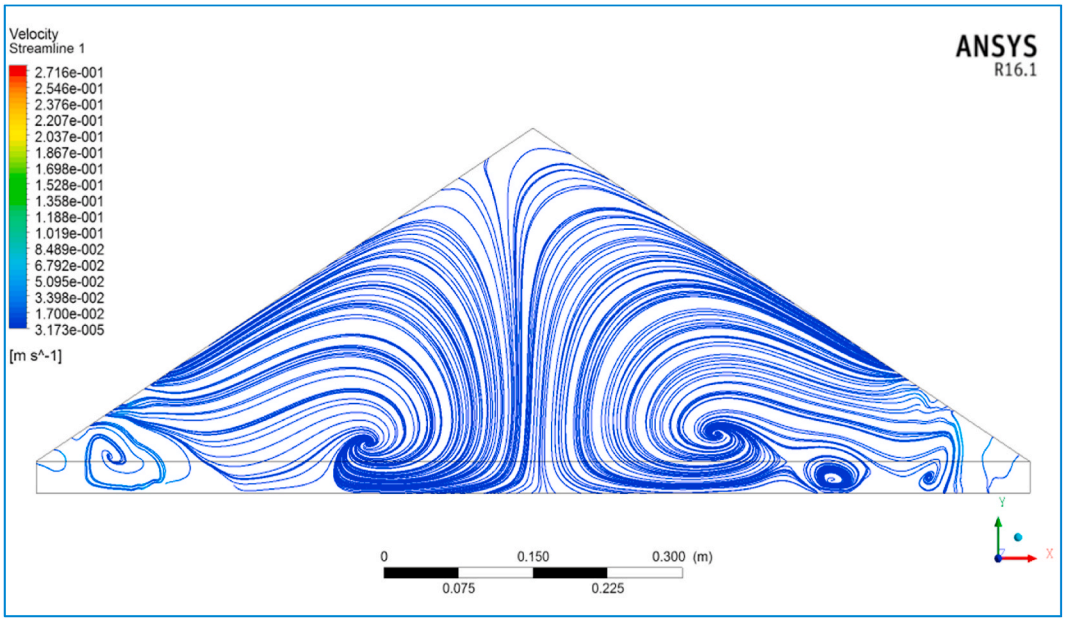

Figure (11). streamline contour for Traditional design still at 12:00 p.m.

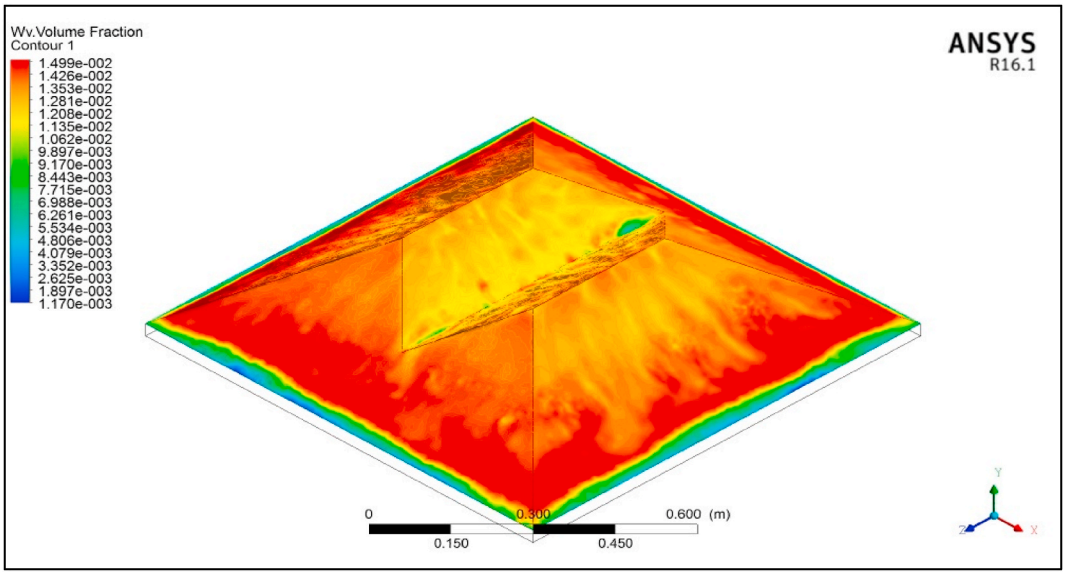

Figure (12). water volume fraction contour for modifying solar still at 12:00 p.m.

1 Modifying, and conventional solar still have had their performance analyzed using both experimental and computational modeling.
2 The efficiency of the developed design can be observed after making a numerical and practical comparison with the traditional design and also comparing it with other studies.
3 This design of the solar still can be applied in any country around the world while ensuring that the glass cover is tilted with the latitude circles of that region
4 Increasing the surface area of the absorber plate by 20 % by making slices along its length, and changing the shape of the glass cover led to an increase in the productivity and efficiency of the developed solar still.
5 Changing the shape of the glass cover resulted in reducing the size of the air gap from 1.245 m3 to 1.112 m3, while maintaining the condenser surface area.

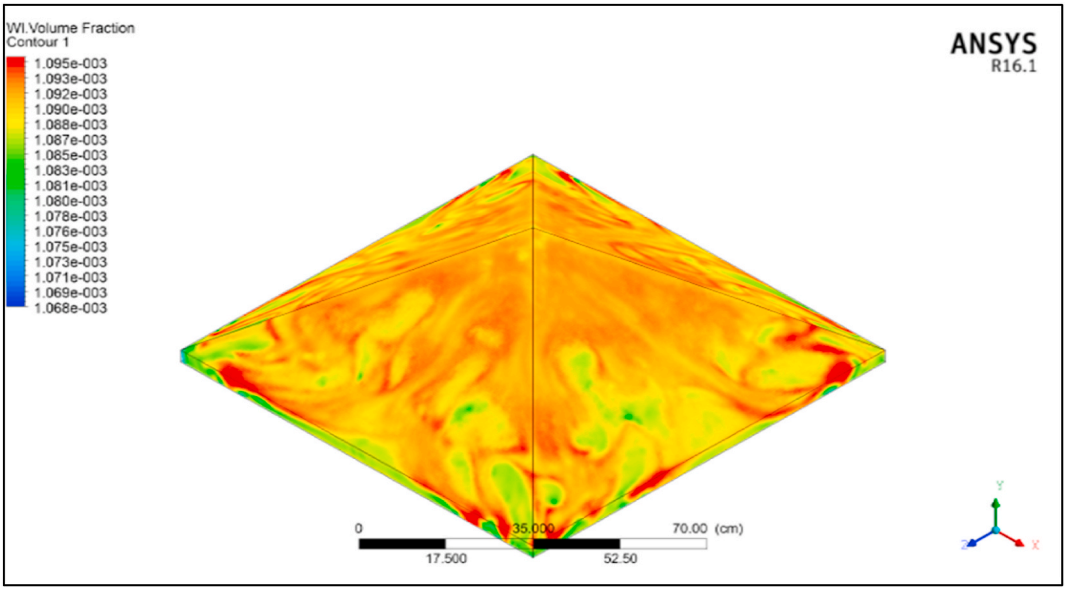

Figure (13). water volume fraction contour for Traditional solar still at 12:00 p.m.

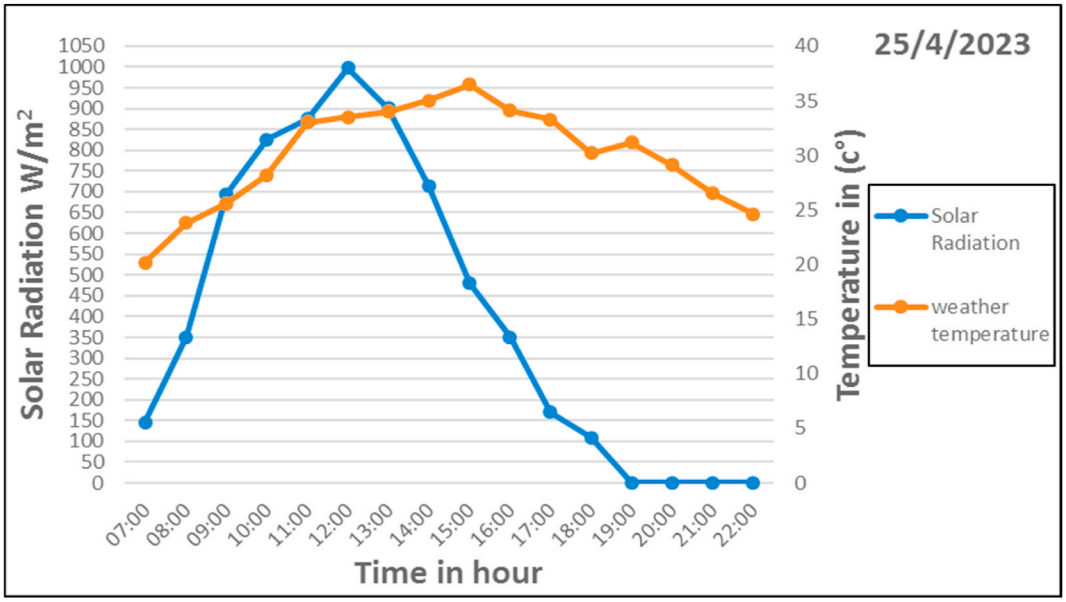

Figure (14). ambient temperatures and solar radiation on the test day.

6 The solar system's productivity and solar radiation intensity are directly related, with productivity and efficiency rising as the radiation intensity rises. as the sun sets, they get smaller,
7 The amount of heat lost from the still is greatly affected by wind speed and the temperature of the surrounding air.
8 Similar to how more absorbent plate surface area improves production, more condensation surface area does the same.
9 New design of the solar distiller is more productive 4.4 l m^{-1} l^{-1} than the conventional pyramid solar still 2.6 l $m^{-1}d^{-1}$.
10 Efficiency of new design increased by 73 % compared with CSS.

Future Recommendations

1. Since glass is breakable, I recommend using materials that have the characteristics of glass and at the same time have the breakage resistance of plastic.

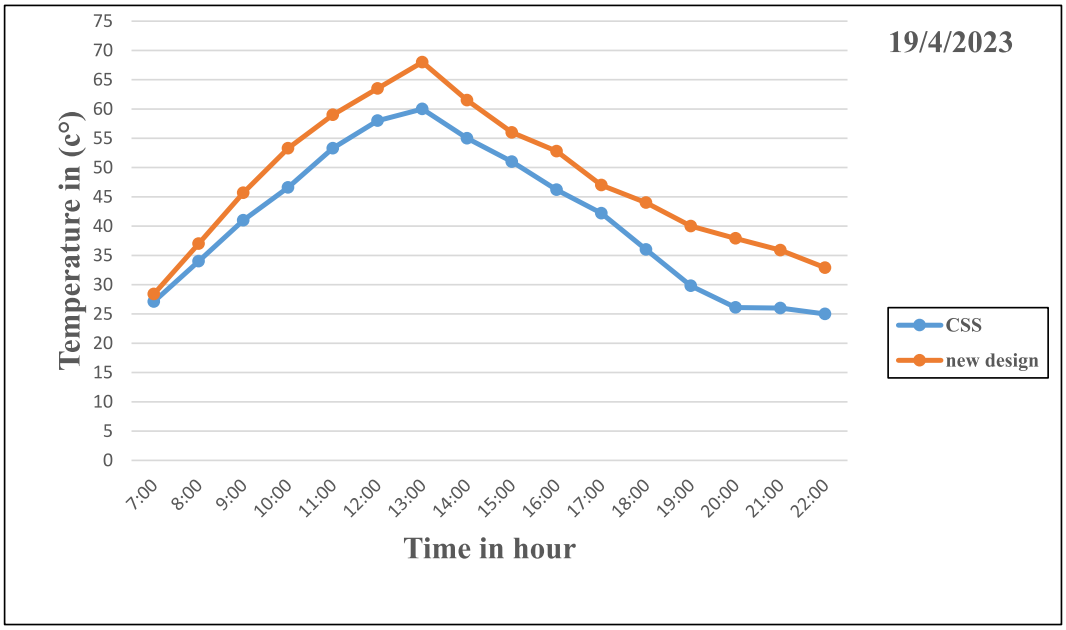

Figure (15). water Temperature for conventional, modified solar still.

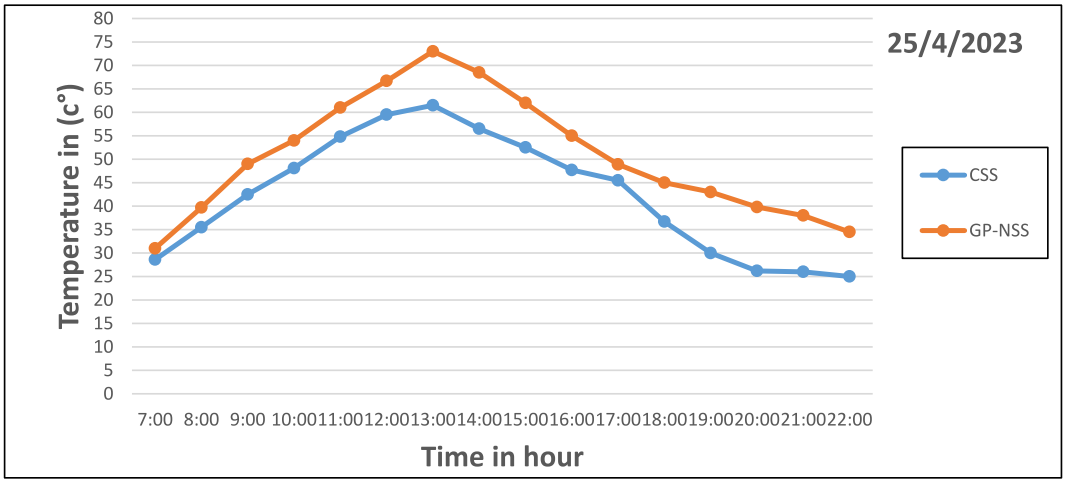

Figure (16). Basin Temperature for conventional, modified solar still solar still.

2. Examine the solar still in all seasons of the year and make a comparison of the distillery's productivity, not relying on one season of the year.
3. Conduct an economic feasibility study of the total cost of the solar still, since the current study did not study the economic aspect.
4. One of the problems that the researcher faced was the dust that collects on the surface of the glass cover, thus reducing the permeability of the glass. Therefore, I recommend making a self-cleaning system.

Additional information

No additional information is available for this paper.

CRediT authorship contribution statement

Abbas S. Shareef: Supervision. **Hayder J. Kurji:** Supervision. **Ahmed H. Hamzah:** Writing - review & editing, Writing - original draft, Visualization, Validation, Software, Resources, Project administration, Methodology, Investigation, Funding acquisition, Formal analysis, Data curation, Conceptualization.

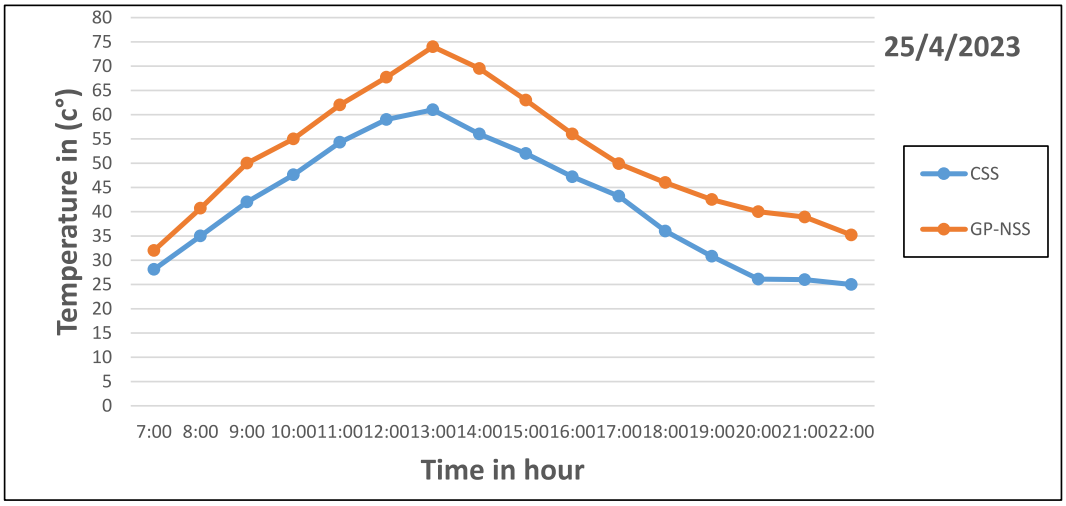

Figure (17). Vapor temperature for conventional, modified solar still solar still.

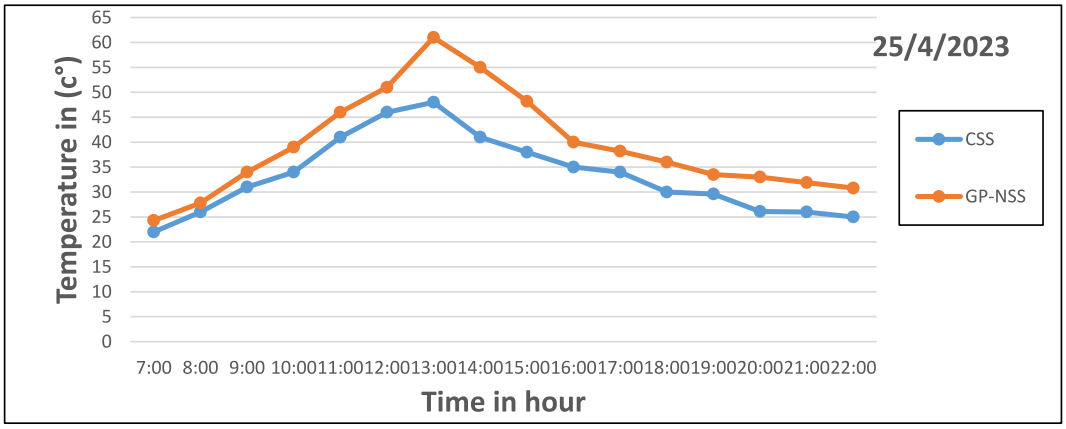

Figure (18). inner glass temperature for conventional, modified solar still solar still.

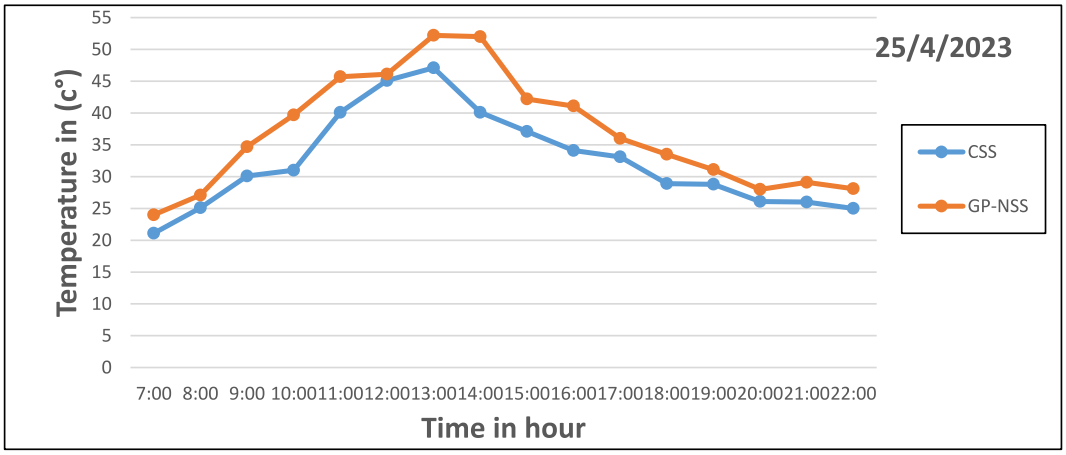

Figure (19). outer glass temperature for conventional, modified solar still solar still.

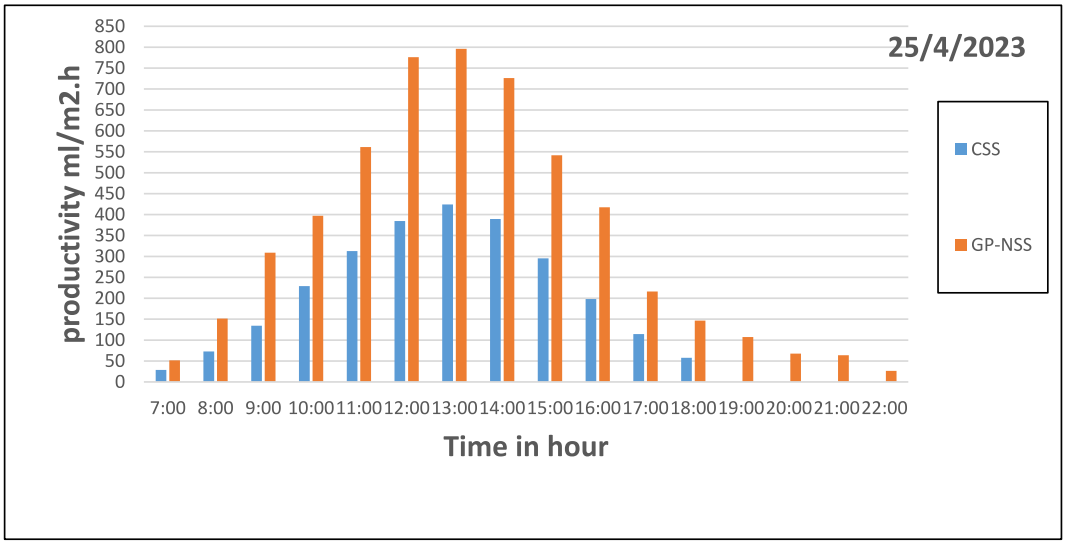

Figure (20). Hourly Productivity for conventional, modified solar still solar still.

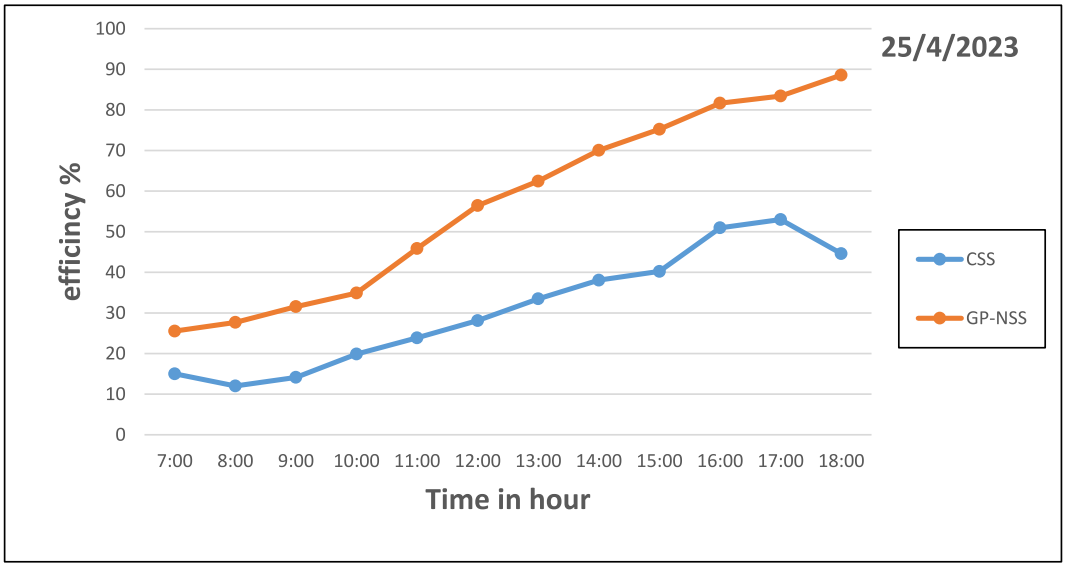

Figure (21). Hurly thermal efficiency for conventional, modified solar still solar still.

Declaration of competing interest

The authors declare that they have no known competing financial interests or personal relationships that could have appeared to influence the work reported in this paper.

Acknowledgements

The authors are grateful for the financial support towards this research by the mechanical Engineering Department, College of Engineering, kerbala University. Postgraduate.

NOMENCLATURE

GP-NSS	Graphite Panel Nanoparticles Solar Still
CSS	conventional Solar Still
A	Area, mˆ2

Cp	Specific heat capacity, J/(kg °C)
D	Cylinder diameter, m
g	Gravitational constant, m/sˆ2
h	Heat transfer coefficient, W/(mˆ2 °C)
k	Thermal conductivity, W/(m °C)
Nu	Nusselt number
Q	Input heat, W
Ra	Rayleigh number
R_{th}	Thermal resistance, °C/W
T	Temperature, °C

Greek symbols

α	Thermal diffusivity, mˆ2/s
β	Expansion coefficient, 1/K
μ	Dynamic viscosity, kg/(m s)
ν	Kinematic viscosity, mˆ2/s
ρ	Density, kg/mˆ3
ε	Emissivity

References

[1] S.K. Shukla, V.P.S. Sorayan, Thermal modeling of solar stills: an experimental validation, Renew. Energy 30 (5) (2005) 683–699.
[2] A.A. El-Sebaii, M. El-Naggar, Year round performance and cost analysis of a finned single basin solar still, Appl. Therm. Eng. 110 (5) (2017) 787–794.
[3] J. Karlsson, A. Roos, Modelling the angular behavior of the total solar energy transmittance of windows, Sol. Energy 69 (2000) 321–329.
[4] Y. Taamneh, M.M. Taamneh, Performance of pyramid-shaped solar still: experimental study, Desalination 291 (2012) 65–68.
[5] A. Kianifar, Saeed Zeinali Heris, Omid Mahian, Exergy and economic analysis of pyramid-shaped solar water purification system: active and passive cases, Energy 38 (2012) 31–36.
[6] G.N. Tiwari, J.M. Thomas, E. Khan, Optimisation of glass cover inclination for maximum yield in a solar still, Heat Recover Syst CHP 14 (1994) 447–455.
[7] A.A. El-Sebaii, Effect of wind speed on some designs of solar stills, Energy Convers. Manag. 41 (2000) 523–538.